Click to view slide presentation

Effect of Stress Anisotropy on Borehole Failure Initiation and Extent: A Laboratory Experimental Observation*

Bailin Wu[1], Xavier Choi[1,2], and Ranjith Pathegama Gamage[2]

Search and Discovery Article #42290 (2018)**
Posted October 8, 2018

*Adapted from extended abstract prepared in conjunction with oral presentation given at 2018 AAPG Asia Pacific Region GTW, Pore Pressure & Geomechanics: From Exploration to Abandonment, Perth, Australia, June 6-7, 2018
 DOI:10.1306/42290Wu2018

[1]CSIRO Energy, Melbourne, Australia (bailin.wu@csiro.au)
[2]Department of Civil Engineering, Monash University, Melbourne, Australia

Abstract

It is a common knowledge that failure of an open hole is affected by anisotropy of the two far field principal stresses acting perpendicular to the borehole, and to some less extent, by the principal stress acting parallel to the borehole. This knowledge is utilized in designing oil and gas well trajectory, wherever possible, to orient the borehole in the direction that minimizes the stress anisotropy. Linear elasticity, coupled with a strength criterion, such as Mohr – Coulomb strength criterion, is routinely applied to assess borehole stability and sand production. It is well known that such a simplistic model is, in mostly cases, overly conservative and requires field (preferred) or laboratory calibration. The calibrated model is then applied to the boreholes oriented in the other directions. For example, for borehole stability analyses, the model would be firstly calibrated on a vertical exploration well, and the calibrated model is then applied to analyze borehole stability for deviated or horizontal development wells, taking into account other geomechanics factors likely to have an impact on the stability of the borehole, such as rock formation anisotropy, faults, and natural discontinuities. In general, formation rock mechanical behavior is far more complex than that the idealistic linear elasticity can describe. Although the calibration process will simplify most of this complexity, it remains questionable how reliable such a calibrated model is when applied to the boreholes with different orientations, hence, different stress anisotropies. Field evidence suggests that under a normal fault stress regime, the stability of a horizontal well may not be very sensitive to well orientation (Morita, 2004 and Wu and Tan, 2010).

To gain a better understanding on the effect of stress anisotropy on borehole stability, we performed a comprehensive literature review on available laboratory borehole stability/borehole breakout experiments under true 3D stress conditions. In comparison with field observation and experience on borehole stability, the advantage of laboratory experiments is obvious; the properties of the rock specimen can be well characterized, the boundary stresses are accurately controlled, borehole conditions are monitored, and failure initiation and extent can be accurately determined.

Discussion

Over 170 data sets were collected from polyaxial cell experiments on block specimens on synthetic sandstones, natural sandstones, limestones and granite. In all the experiments, the borehole was not supported, and the rock specimen was at least 5 times of the borehole diameter. The method to identify borehole failure and stabilization included acoustic emission (AE), borehole deformation/strain, and real time visual observation. A considerable portion of the data sets included borehole failure initiation and borehole breakout stabilized stress conditions with measurements on breakout width and depth. Table 1 summarizes the experimental conditions, rock types, specimen and borehole dimension, and methods for identifying borehole failure initiation and borehole breakouts and data sources covered by this review.

The experimental data were analyzed based on the conventional borehole stability model, i.e., linear elasticity and Mohr-Coulomb strength criterion (M-C). For borehole failure initiation, it is assumed that the stress condition at point A (Figure 1) satisfies the strength criterion, i.e.,

$$\frac{\sigma_H}{\sigma_C}\frac{3K-1}{K} = 1 \qquad \text{Equation 1}$$

where σ_C is the borehole strength calibrated at point A for a hydrostatic or a lower anisotropic stress condition, and K is the ratio of σ_H/σ_h. The data set of experimental borehole stability is analyzed based on Equation 1 and presented in Figure 2. Despite the scatter of the experimental data, not unexpected from the diverse sources of the data and rock types, the general trend in Figure 2 demonstrates that the conventional borehole stability model calibrated at a hydrostatic or lower anisotropic stress condition would underestimate the borehole strength with a higher stress anisotropy.

It would be interesting to understand if the calibrated conventional borehole stability model based on borehole failure initiation condition can be used to estimate the borehole failure extent, i.e., breakout width and depth. The breakout width may be estimated from the stress and strength condition at points B or C (Figure 1) as,

$$2\phi_b = 180 - acos\left[\frac{(K+1)-\sigma_c/\sigma_h}{2(K-1)}\right] \qquad \text{Equation 2}$$

The breakout width calculated from Equation 2 is compared with the experimental data in Figure 3, which shows that the calibrated analytical model may be used to estimate the breakout width, in comparison with the uncalibrated model (i.e., with the laboratory measured UCS). The uncalibrated model, in general, overly estimates the breakout width.

The breakout depth may be estimated from the stress and strength condition at point D in Figure 1. The normalized breakout depth can be obtained from the solution of Equation 3 below,

$$\frac{3(\sigma_H-\sigma_h)}{1-\sin\phi}\left(\frac{R}{r}\right)^4 + \left[\frac{1+\sin\phi}{1-\sin\phi}\frac{(-3\sigma_H+5\sigma_h)}{2} + \frac{(\sigma_H+\sigma_h)}{2}\right]\left(\frac{R}{r}\right)^2 + \sigma_H - \sigma_C - \frac{1+\sin\phi}{1-\sin\phi}\sigma_h = 0 \qquad \text{Equation 3}$$

The breakout depth calculated from Equation 3 is compared with the experimental data in Figure 4. In comparison, the calibrated conventional borehole stability model underestimates the borehole breakout depth of the measured experimental data, i.e., the borehole breakout depths estimated from the analytical model is too shallow. It is interesting to note that the uncalibrated model (i.e., use of laboratory measured UCS) can give a better estimation on the borehole breakout depth than the calibrated model.

Based on the review over 170 sets of borehole stability experimental data under a 3D stress conditions and the limited analyses using the conventional borehole stability model, it may be concluded:

- The conservativeness of the model of linear elasticity coupled with the Mohr-Coulomb strength for borehole stability analyses has been confirmed under 3D stress conditions, hence the model needs calibration;
- The calibrated model at a lower stress anisotropy may underestimate borehole strength (failure initiation condition) with a higher stress anisotropy;
- The calibrated model may be applied to estimate borehole breakout width, but may not for the breakout depth, i.e., the estimated borehole breakout depth may be too shallow in comparison with the experimental data;
- One of the major drawbacks with the existing borehole stability model is that the Kirsch solution for a perfect circular hole is applied, which is not valid once borehole failure starts. Development of accurate stress solution for boreholes with breakouts is currently on-going.

References Cited

Addis, M.A., N.R. Barton, S.C. Band, and J.P. Henry,1990, Laboratory Studies on the Stability of Vertical and Deviated Boreholes: SPE-20406-MS, 65th Annual Technical Conference and Exhibition, Society of Petroleum Engineers, New Orleans, LA. September 23-26. doi.org/10.2118/20406-MS

Cheon, D.S., S. Jeon, C. Park, W.K. Song, and E.S. Park, 2011, Characterization of Brittle Failure Using Physical Model Experiments Under Polyaxial Stress Conditions: International Journal of Rock Mechanics and Mining Science, v. 48, p. 152-160.

Haimson, B.C., and C.G. Herrick, 1986, Borehole Breakouts – A New Tool for Estimating in Situ Stress?: Proceedings International Symposium on Rock Stress and Rock Stress Measurements, Stockholm, 1-3 September, p. 271-280.

Haimson, B.C., and I. Song, 1993, Laboratory Study of Borehole Breakouts in Cordova Cream: A Case of Shear Failure Mechanism: International Journal of Rock Mechanics and Mining Science & Geomechanics Abstracts, v. 30/7, p. 1047-1056.

Herrick, C.G., and B.C. Haimson, 1994, Modeling of Episodic Failure Leading to Borehole Breakouts in Alabama Limestone *in* P.P. Nelson and S.E. Lauback (eds.), Rock Mechanics, Balkema, Rotterdam, ISBN 90 5410 380 8.

Lee, M., and B.C. Haimson, 1993, Laboratory Study of Borehole Breakouts in Lac du Bonnet Granite: A Case of Extensile Failure Mechanism: International Journal of Rock Mechanics and Mining Science & Geomechanics Abstracts: v. 30/7, p. 1039-1045.

Morita, N., T. Doi, and T. Kinoshita, 2002, Stability of an Open hole Completed in a Limestone Reservoir with and Without Acid Treatments: SPE 77776-MS, SPE Annual Technical Conference and Exhibition, San Antonio, Texas, 29 September - 2 October, 15 p. doi.org/10.2118/77776-MS

Morita, N., 2004, Well Orientation Effect on Borehole Stability: SPE-89896-MS, SPE Annual Technical Conference and Exhibition, Houston, Texas, 26-29 September, 12 p. doi.org/10.2118/89896-MS

Papamichos, E., J. Tronvoll, A. Skjaerstein, and T. Unander, 2010, Hole Stability of Red Wildmoor Sandstone Under Anisotropic Stresses and Sand Production Criterion.: Journal of Petroleum Science and Engineering, v. 72/1-2, p. 78-92.

Villarroel, F.M.G., V.A. De Azevedo, G. Rabello, M. Bloch, and E. Vargas Jr., 2010, Breakouts: Physical, Numerical and Analytical Modeling: SPE-131656-MS, SPE EUROPEC/EAGE Annual Conference and Exhibition, 14-17 June, Barcelona, Spain, 9 p. doi.org/10.2118/131656-MS

Wu, B., S.K. Choi, and C.P. Tan, 2005, Effect of Stress Anisotropy on Cavity Strength and Implications in Wellbore Stability and Sand Production Analyses: ARMA/USRM 05-773, 40th US Rock Mechanics Symposium: Rock Mechanics for Energy, Mineral and Infrastructure Development in the Northern Regions, Anchorage, Alaska, 25-29 June.

Wu, B., and C.P. Tan, 2010, Effect of Shale Bedding Plane Failure on Wellbore Stability – Example from Analyzing Stuck-Pipe Wells: ARMA 10-350, 44th US Rock Mechanics Symposium and 5th U.S.-Canada Rock Mechanics Symposium, Salt Lake City, UT, 27-30 June.

Younessi, A., V. Rasouli, and B. Wu, 2013, Sand Production Simulation Under True-Triaxial Stress Conditions: International Journal of Rock Mechanics and Mining Science, v. 61, p. 130-140.

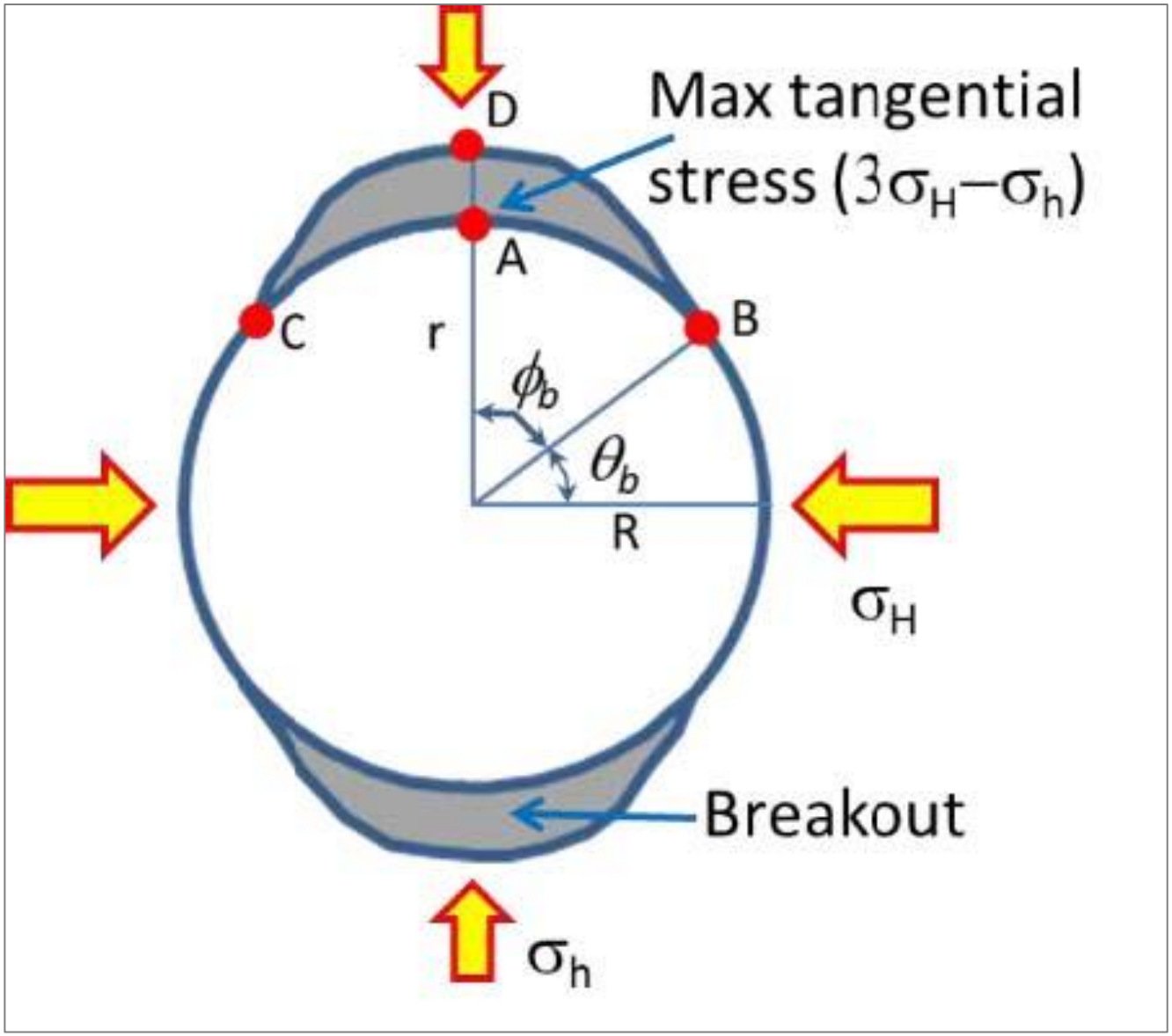

Figure 1. Conventional borehole stability analysis model.

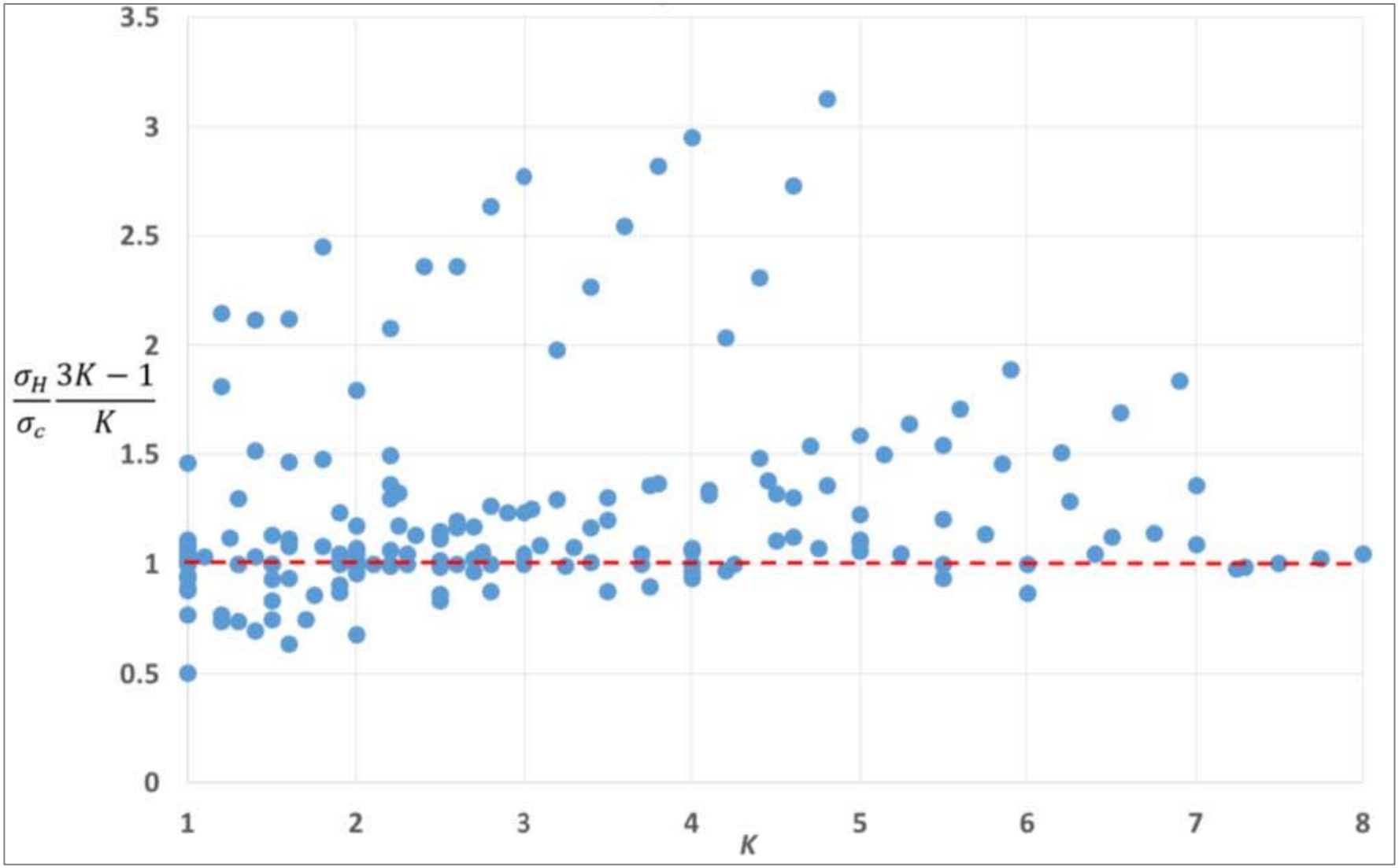

Figure 2. Comparison of calibrated analytical model with experimental data – borehole failure initiation.

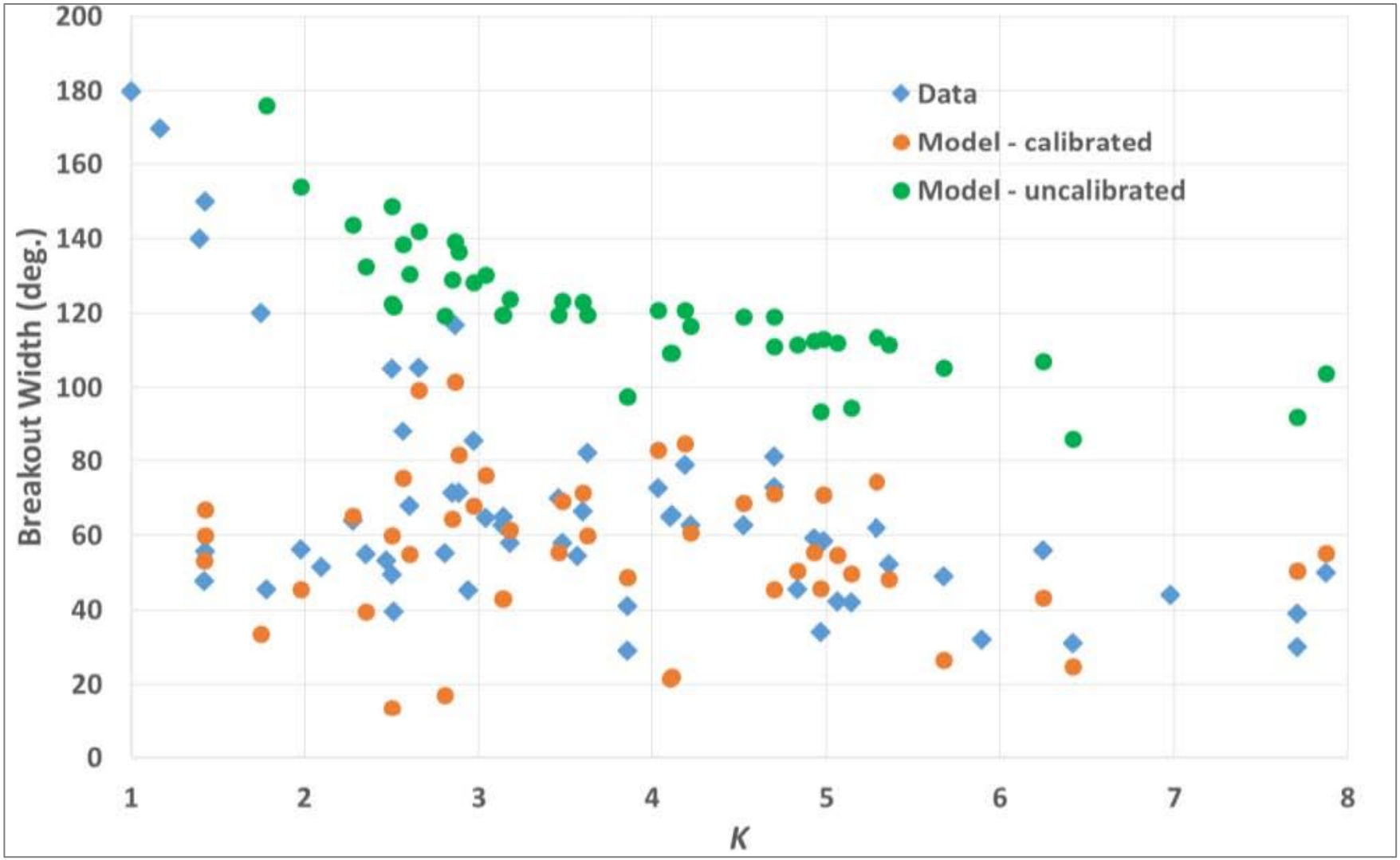

Figure 3. Comparison of calibrated analytical model with experimental data – borehole breakout width.

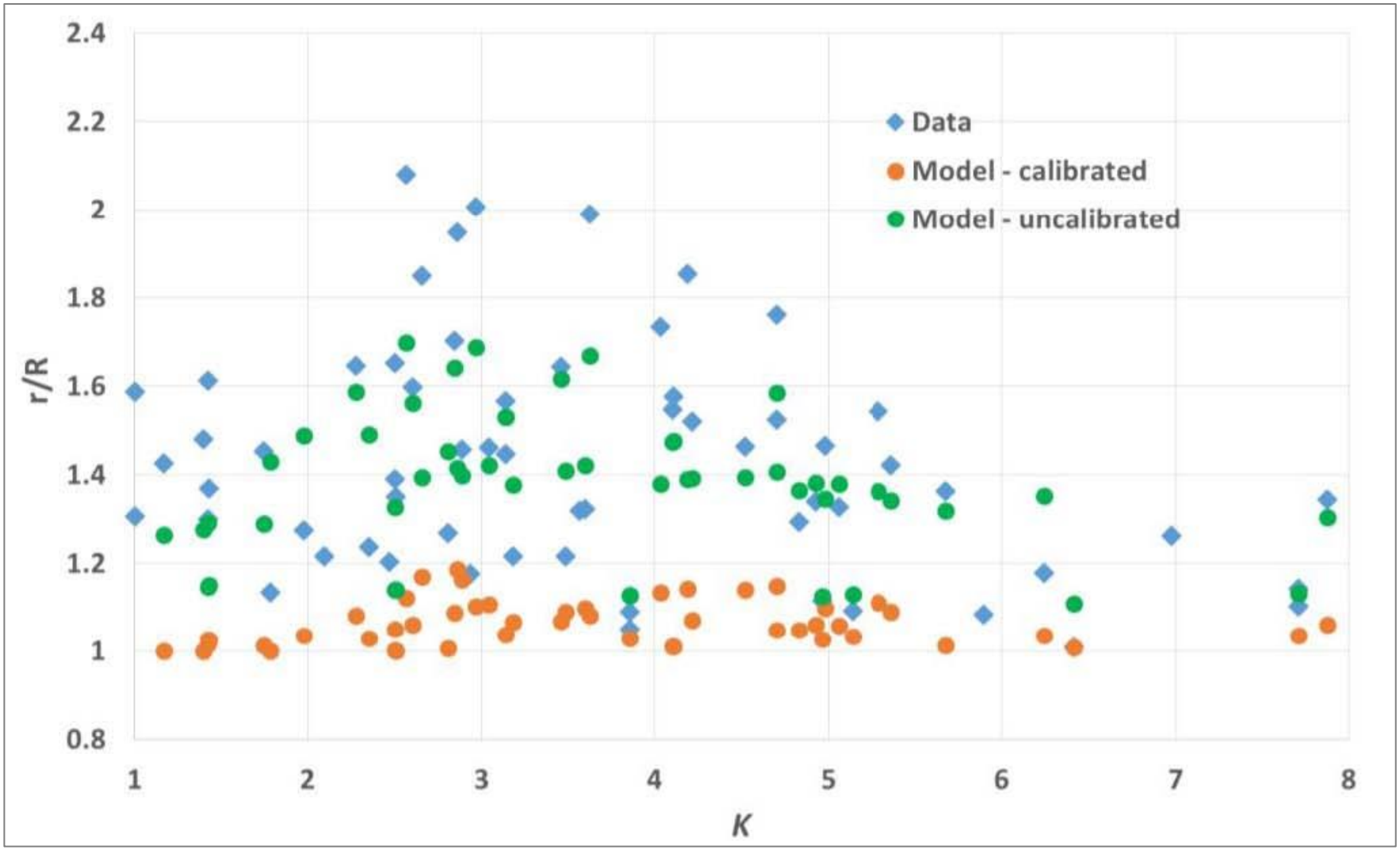

Figure 4. Comparison of calibrated analytical model with experimental data – breakout depth.

Specimen size (mm)	Borehole size (mm)	Failure detection method	Rock type	UCS (MPa)	Reference
130x130x130	21.4	Borehole strain and AE (to check)	Indiana limestone	27.7 (dry) 25 (saturated)	Haimson & Herrick 1986
500 & 400 cubes	50.8	Borehole deformation, sensors & AE	Synthetic & Gres des Vosges sandstones	0.5 & 24.4	Addis et al 1990
130x130x130	22	Borehole strain and AE	Cordova limestone	21 & 13 (normal & parallel to bedding)	Haimson and Song 1993
100x100x100	21	Borehole deformation, AE & video camcorder	Lac du Bonnet Granite	167	Lee & Haimson 1993
130x130x170	11	Borehole strain and AE	Alabama limestone	42.7 (inferred from *c* and □)	Herrick & Haimson 1994
267x267x267	60	Borehole deformation	Limestone	32.5	Morita 2004
267x267x445	57	Borehole deformation	Limestones & castlegate	32.5, 12 & 6.5	Morita et al. 2002
85x85x100	17	Borehole deformation & borehole camera	CG & MF sandstones	8.3 & 0.8	Wu et al 2005
60x60x70	15	Borehole deformation	Red Wildmoor sandstone	11.3	Papamichos et al 2010
300x300x300	60	Webcam	Synthetic sandstone	9.06	Villarroel et al 2010
290x290x290	60	AE	Synthetic sandstone	38	Cheon et al 2011
100x100x100	15	Borehole camera	Synthetic sandstone	6	Younessi et al 2013

Table 1. Summary of the experimental conditions, rock type and strength, and data sources.

Click to view slide presentation.